ELSEVIER

Coordination Chemistry Reviews 230 (2002) 49–64

COORDINATION CHEMISTRY REVIEWS

www.elsevier.com/locate/ccr

Bonding and structural preferences of indenyl complexes: $MInd_2L_n$ ($n = 0$–3)

Maria José Calhorda [a,*], Vitor Félix [b], Luís F. Veiros [c]

[a] *Departamento Química e Bioquímica, Faculdade de Ciências, Universidade de Lisboa, ITQB, Av. da República, EAN, Apt 127, 2781-901 Oeiras, Portugal*

[b] *Departamento Química e Bioquímica, Faculdade de Ciências, Universidade de Lisboa, 1749-016 Lisboa, Portugal*

[c] *Centro de Química Estrutural, Complexo I, Instituto Superior Técnico, Av. Rovisco Pais, 1, 1049-001 Lisboa, Portugal*

Received 30 November 2001; accepted 4 March 2002

Dedicated to Professor Derk J. Stufkens on the occasion of his retirement

Contents

Abstract . . . 49
1. Introduction . . . 49
2. Methods . . . 50
3. Results and discussion . . . 50
   3.1 The coordination modes of indenyl . . . 50
   3.2 $MInd_2$ compounds . . . 51
   3.3 $MInd_2L_2$ compounds . . . 55
   3.4 $MInd_2L_n$ ($n = 1$, 3) compounds . . . 61
4. Conclusions . . . 62
5. Computational details . . . 62
Acknowledgements . . . 62
References . . . 62

Abstract

A search of bis(indenyl) derivatives available in the Cambridge Crystallographic Data Centre was performed and the two main families, $MInd_2$ and $MInd_2L_n$ ($n = 1$–3), were structurally analyzed in detail. DFT calculations were performed for some relevant compounds in order to understand their electronic structure and interpret the experimental data. For $MInd_2$ complexes, the rotation angles between the rings show a wide range of values, depending both on the electron count and on the steric effects of the ring substituents. Hapticity change toward η^3 is induced by extra electrons, but a perfect η^3 coordination is never observed. For the electron deficient Cr(II) complexes, two isomers having two and four unpaired electrons are known for different substituents, and the calculated energies in models are very close, as expected. The $MInd_2L_2$ family is the largest one and examples of η^3 coordination can be found. Both electronic and steric effects play a major role in determining the structural parameters of these species, but in the absence of bulky ring substituents, the rings are fluxional.

Keywords: Indenyl; Metallocenes; Crystal structures; Hapticity; DFT calculations

1. Introduction

Complexes containing the indenyl ring as a ligand have received much attention owing to the 'indenyl effect', as defined by Basolo et al., who noticed that replacement of a cyclopentadienyl ring ($Cp = C_5H_5^-$) by an indenyl ring ($Ind = C_9H_7^-$) led to strongly accelerated

* Corresponding author. Tel.: +351-21-446-9754; fax: +351-21-441-1277

E-mail address: mjc@itqb.unl.pt (M.J. Calhorda).

0010-8545/02/$ - see front matter
PII: S0010-8545(02)00081-4

reaction rates [1]. The family of homoleptic bis(indenyl) derivatives comprises a small number of complexes; most of them derive from Fe, Co, and Ni, and their electronic structure was studied in a recent work [2]. When the metal is less electron rich, it has an increased tendency to add more ligands and form species $MInd_2L_n$ ($n = 0$–3). Among this group, the zirconium derivatives, and specially the ansa-metallocenes, where the two indenyl groups are held together by a bridge, play a special role in Ziegler–Natta polymerization [3] and have thus been much studied [4]. The formally Zr(IV) complexes typically contain two L groups and have a 16 electron count (L will denote both neutral and anionic ligands throughout this work). As one moves to molybdenum, with two more electrons, reactions of Mo(IV) or Mo(II) species will easily give rise to formally 20 electron intermediates. To avoid them, the η^5-coordinated indenyl may slip and become η^3-coordinated, keeping the stoichiometry. Such processes, following ligand addition or reduction, have been studied for several systems, both from an experimental [5] and a theoretical [6] point of view. One important aspect is the structural rearrangement of the molecule which takes place in many systems upon ring slippage, namely when an indenyl and a cyclopentadienyl are present [6j,6k,6l,6m,6n,6o]. In order to have a complete overview of the structural changes accompanying haptotropic shifts for the bis(indenyl) derivatives with non-linked rings, a search in the Cambridge Crystallographic Data Centre (CCDC) was performed [7] and the results will be discussed and analyzed, so that the role of electronic and steric effects can be determined. DFT calculations [8] were performed in order to explain the structural preferences of the compounds. It should be noticed, however, that substituents are usually not included in the model compounds studied, giving rise in some cases to discrepancies between calculated and experimental structures.

2. Methods

The solid state structures of bis(indenyl)metal complexes are reviewed, based on X-ray single crystal determinations available from Cambridge Crystallographic Data Centre (upgrade, April 2001) [7]. Complexes $MInd_2$ and $MInd_2L_n$ ($n \geq 1$) are covered. M represents any metal of the Periodic Table π-bonded to the indenyl ligand exclusively through carbons atoms of the five-member ring, while L is a mono or bidentate ligand. However, metal complexes with other polyenyl ligands exhibiting η^2 or higher hapticities are excluded. In addition, the metal complexes in which the indenyl ring is part of an *ansa* ligand are also excluded (they have been studied in detail [4]), as well as those where the metal bonded to the indenyl ring is involved in a metal–metal bond. Structures with these connectivities exhibit specific stereoelectronic features requiring a particular study, which is out of the aims of this review. Following these criteria, a significant number of structures were retrieved from the CCDC. In these structures, the indenyl system exhibits ring slippages consistent with coordination modes ranging from η^1 to η^5.

3. Results and discussion

3.1. The coordination modes of indenyl

The indenyl ring can bind through the five carbon atoms in the C_5 ring, giving rise to the η^5 coordination mode, which is usually distorted and can therefore be described as $\eta^2+\eta^3$ as seen in Scheme 1, also showing the atom numbering scheme of indenyl. The difficulty in observing a perfect η^5 coordination for indenyl compounds, contrarily to cyclopentadienyl ones, is assigned to the different contributions of carbon atoms to the indenyl π orbitals, owing to the presence of the benzene ring [2a]. The $\eta^2+\eta^3$ description emphasizes this aspect, although the ring exhibits an overall η^5 hapticity.

Several structural parameters can be used to define the indenyl coordination, namely the M–C distances and the folding angle Ω (HA), defined as the angle between the planes of carbons [C(1), C(2), C(3)] and [C(1), C(3), C(4), C(9)] [6]. Some authors also consider the angle made by the planes of the pentagon [C(1), C(2), C(3), C(4), C(9)] and the hexagon [C(4), C(5), C(6), C(7), C(8), C(9)] (FA) [9]. The distinction between these two angles is that the first one gives the bending along the C(1)–C(3) line, while the second describes the bending at the C(4)–C(9) ring junction. The M–C distances characterize the slip distortion; the slip parameter (ΔM–C), defined as the difference between the average distance from the metal center to the carbon atoms shared by both six- and five-membered rings (C(4) and C(9)) and the average distance from the metal to the adjacent carbon atoms, C(1), C(2), and C(3), will be used (Scheme 2).

These parameters and the corresponding nomenclature, proposed for the first time by Faller et al. [5l] have been extensively used to characterize the coordination mode of indenyl in complexes. However, the folding angle Ω and the slip parameter ΔM–C show the most straightforward relationship with $\eta^3 \rightarrow \eta^5$ indenyl slip-

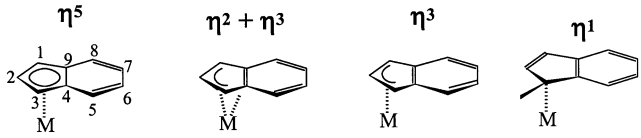

Scheme 1.

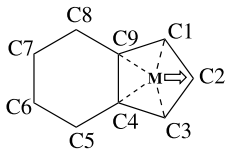

Scheme 2.

Table 1
Structural data for $MInd_2$ complexes (distances in Å, angles in °)

Complex	Refcode	RA	HA	ΔM–C	ΔM–C′
[$FeInd_2$]	DINDFE01	13.0	2.6	0.049	0.050
	DINDFE01	5.5	2.0	0.033	0.039
[$FeInd''_2$]	FACXOW	73.4	1.3	0.016	0.039
[$RuInd_2$]	INDERU	0.5	1.7	0.024	0.037
[$FeInd'_2$]	PUHPIR	35.1	2.7	0.042	0.049
[$FeInd^*_2$]	VILWES	151.3	2.4	0.030	0.030
[$FeInd^*_2$]	PITLUZ	97.4	4.1	0.068	0.080
[$CoInd^*_2$]$^+$	YALNUU	91.3	5.4	0.060	0.057
	YALNUU	90.6	3.9	0.059	0.049
[$PbInd'_2$]	NEBQUG	101.3	3.6	0.087	0.079
	NEBQUG	97.2	4.6	0.137	0.033
[$CoInd_2$]	VILVUH	10.7	7.3	0.116	0.134
[RhIndInd′]	HAFDEX	17.3	5.3	0.092	0.084
[$NiInd'_2$]	TIBJOD	180.0	12.8	0.342	0.342
	TIBJOD	180.0	13.7	0.360	0.360
[$NiInd_2$]	VILWAO	175.0	13.6	0.419	0.416
[$FeInd'_2$]$^+$	MINDFE	93.1	4.4	0.074	0.075
[$CrInd^*_2$]$^+$	YALPAC	91.1	5.0	0.010	0.024
	YALPAC	92.2	5.4	0.036	0.020
[$CrInd^*_2$]	YALPEG	180.0	7.2	0.098	0.098
[$CrInd'_2$]	[14]	174.7	2.4	0.160	0.138

page and consequently the values of these two parameters will be mainly discussed.

3.2. $MInd_2$ compounds

The structural data concerning $MInd_2$ complexes are collected in Table 1 together with CCDC refcodes. Structures of some representative complexes are given in Fig. 1.

Another relevant structural feature of bis(indenyl)metal complexes is the conformational preference of the two indenyl rings. For simple systems of the type $MInd_2$, the conformation adopted by the two indenyl rings can be described by the RA angle, defined as the dihedral angle between the planes [M, C(2), midpoint of the C(4)–C(9) ring junction] and [M, C(2′), midpoint of the C(4′)–C(9′) ring junction] (Scheme 3). Thus, for a fully eclipsed arrangement of the two indenyl ligands, a RA angle of 0° is expected, while a fully staggered arrangement will correspond to a RA angle of 180°. Alternatively, the torsion angle TA defined as C(2)–Cp_{cent}–Cp'_{cent}–C(2′), where Cp_{cent} and Cp'_{cent} are, respectively, the centroids of the pentagonal rings of the two indenyl ligands, also gives the relative orientation of the two indenyl ligands. In this particular case of $MInd_2$ systems, these two parameters show slight differences. When the two indenyl ligands are parallel, RA is only function of the degree of staggering. However, when the two indenyl rings are not parallel, as in the bent metallocenes $MInd_2LL'$, RA reflects both the degree of ring staggering and the angle between rings. Therefore, for bent bis(indenyl) compounds the RA and TA parameters are significantly different (see Table 2, below) and the relative orientation of two indenyl rings will be described differently.

The first and larger group of complexes in Table 1 is characterized by an 18 electron count and comprises the d^6 metal derivatives, analogues of ferrocene [Fe(II), Ru(II) and Co(III)]. Some substituted indenyl complexes were drawn in Fig. 1, and permethylated indenyl is C_9Me_7 = Ind*.

The indenyl in $FeInd_2$ (two independent molecules in the unit cell) shows unequivocal and almost perfect η^5 coordination, as discussed in detail in Ref. [2a], reflected by folding angles ranging from 2.1 to 2.6° (almost planar) and very small slip parameters (< 0.05 Å). The structure with eclipsed rings has been shown to be the most stable (5 kJ mol^{-1}, from DFT calculations), but this small difference is easily overcome if steric or packing effects play a role, leading to a wide spread of RA angles. Almost perfect eclipsed rings are also observed for $RuInd_2$.

The rotation angle RA can take any values, from 5.5 or 13.0° in $FeInd_2$, to 151.3° in $FeInd^*_2$. The two structures of $FeInd^*_2$ differ strongly in the rotating angle (151.3° for VILWES, 97.4° for PITLUZ), though the other parameters are comparable. The reason lies in different packing effects occurring in PITLUZ, since there is a cocrystallyzed molecule of 7,7′,8,8′-tetracyanoquinodimethene. The rings are arranged in another way, owing to weak C–H···N hydrogen bonds [C–H···N 2.569 Å, 159.5° $(-1/2+x, 1/2-y, 1/2+z)$; C–H···N 2.616 Å, 156.4° $(1-x, -y, -z)$] between the two types of units and π-stacking between rings of the complex and of 7,7′,8,8′-tetracyanoquinodimethene (Fig. 2). In order to take advantage of the space and provide an efficient packing, the rings adopt different conformations.

A RA of 73.4° is observed in [$FeInd''_2$], FACXOW (Fig. 1) and is caused by the steric effects of the bulky substituents of the indenyls, which are minimized in this conformation. A similar effect is seen in the independent molecules of [$CoInd^*_2$]$^+$ (YALNUU) which show RA of ca. 91°.

The Pb derivative, Pb{1,3-$(SiMe_3)_2$-Ind}$_2$, NEBQUG, seems to behave as the previous compounds, as the rings are close to planarity (3.6, 4.6°) and the slip is relatively small (the largest in this group, but close to the others). The rotation angle approaches 100°. However, there are too many electrons in this species, since Pb(II) is

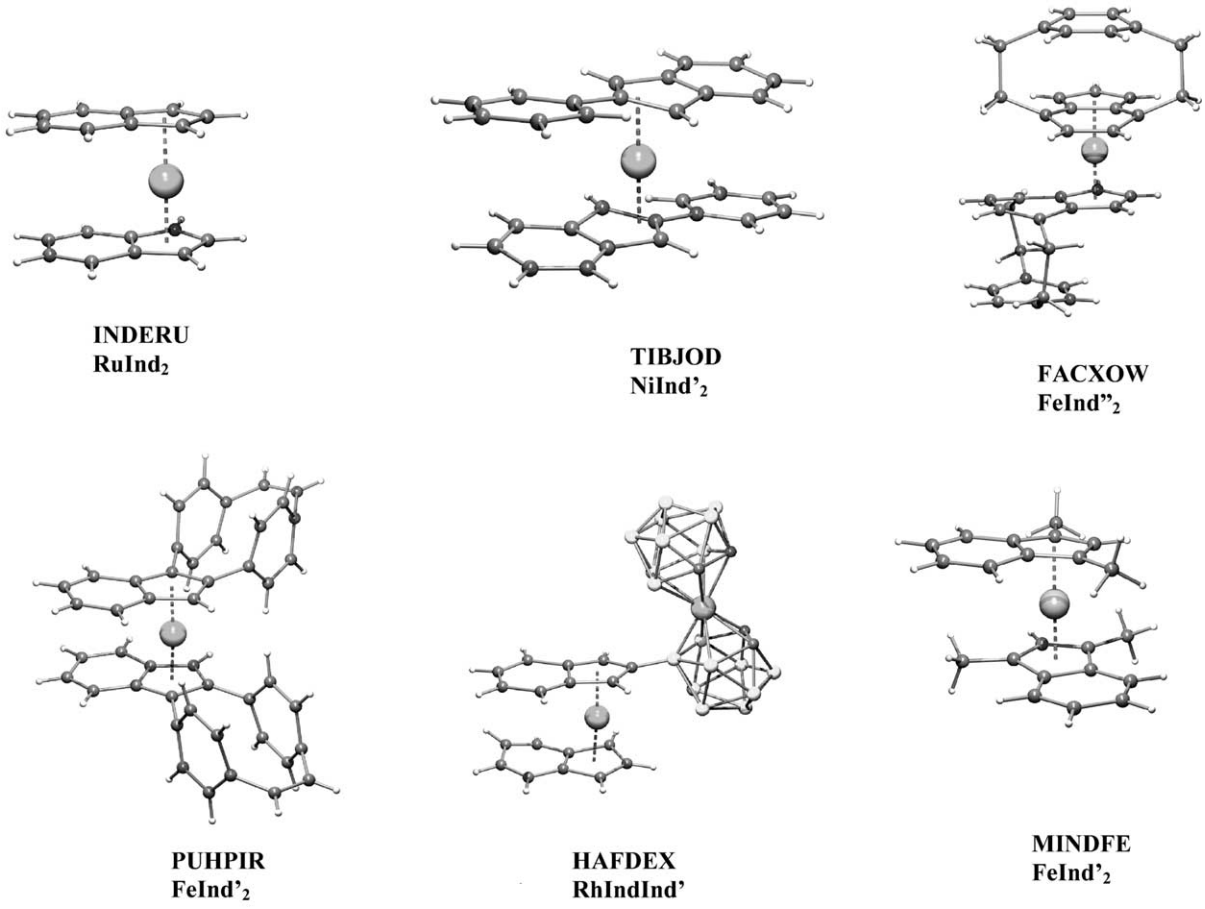

Fig. 1. Molecular structures of some relevant $MInd_2$ complexes featuring eclipsed rings (INDERU), staggered rings (TIBJOD), in between conformations (FACXOW), and other indenyl rings bearing bulky substituents (PUHPIR, HAFDEX, MINDFE). The indenyl hydrogen atoms in HAFDEX, not located in the X-ray structure, were included in the drawing.

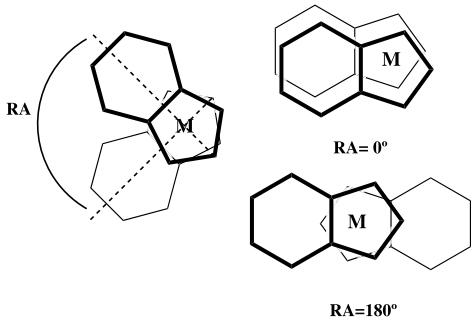

Scheme 3.

formally a $d^{10}s^2$ element [10]. The optimized structure (DFT/B3LYP calculations [11]) of a $PbInd_2$ model shows that the indenyl rings are η^2-coordinated and the angle Cp_{cent}–Pb–Cp'_{cent} is far away from linearity (Scheme 4).

In each ring two carbon atoms are close to Pb, as shown in Scheme 4. The other three distances are 2.83, 2.87, and 2.98 Å, and the two rings are equivalent. This geometric arrangement agrees with the bent structure favored by $PbCp_2$ compounds. Indeed, in a recent paper the trends in structures of, among others, lead metallo-

Table 2
Calculated (DFT) and experimental (NEBQUG) Pb–C distances (Å) in one ring for several structures of the type $PbInd_2$

	$PbInd_2$ (calc.)	$Pb\{1,3\text{-}(SiMe_3)_2\text{-}Ind\}_2$ (calc.)	NEBQUG [b] (exp.) $Pb\{1,3\text{-}(SiMe_3)_2\text{-}Ind\}_2$	
Pb–C(1) [a]	2.60	2.70	2.693	2.720
Pb–C(2)	2.65	2.73	2.712	2.736
Pb–C(3)	2.83	2.89	2.801	2.798
Pb–C(4)	2.98	2.99	2.857	2.812
Pb–C(9)	2.87	2.88	2.795	2.772

[a] See Scheme 1 for numbering scheme.
[b] Two independent molecules in the unit cell.

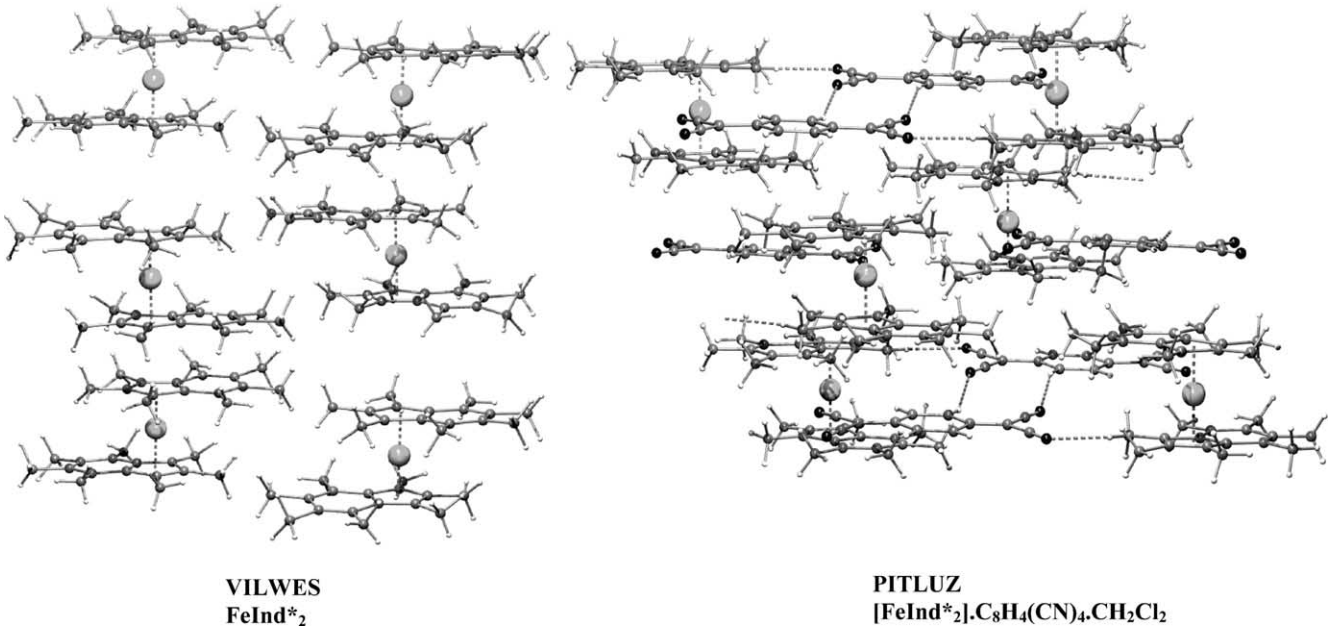

Fig. 2. Packing diagrams for the two $FeInd^*_2$ structures (PITLUZ and VILWES), showing the differences introduced by the cocrystallized molecule.

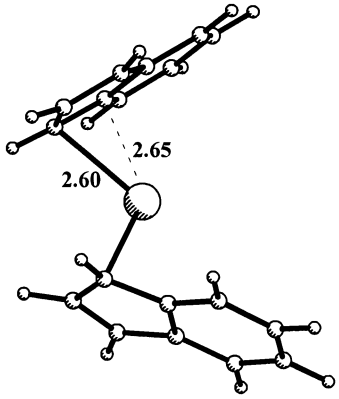

Scheme 4.

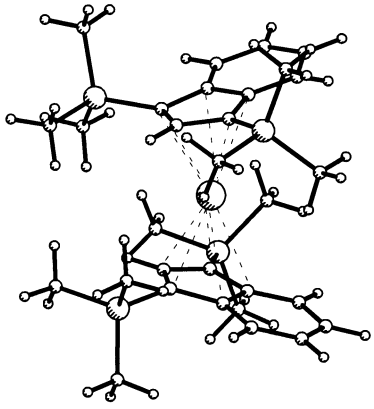

Scheme 5.

cenes was addressed [12]. The authors found that $PbCp_2$ prefers to adopt a bent geometry (Pb–C distances are comparable with ours), but the energy required to make it planar is very small (0.27 kcal mol^{-1}). A full optimization of the complete structure of Pb{1,3-$(SiMe_3)_2$-Ind}$_2$ gives an apparently different result. Indeed, the rings appear to be η^5-coordinated (Scheme 5), since there is not such a spread of Pb–C distances as before, but the distances are longer, as shown in Table 2.

The bulkiness of the two $SiMe_3$ substituents on each ring prevents them from occupying the electronic preferred position and forces the rings to become more parallel. The X-ray observed structure, showing the same effects, is given in Fig. 3.

$CoInd_2$ (VILVUH) is formally a 19 electron species. The extra electron occupies a metal-ring antibonding orbital which drives the slippage of the ring in order to relieve this antibonding character (Scheme 6) [2a,6j,6o].

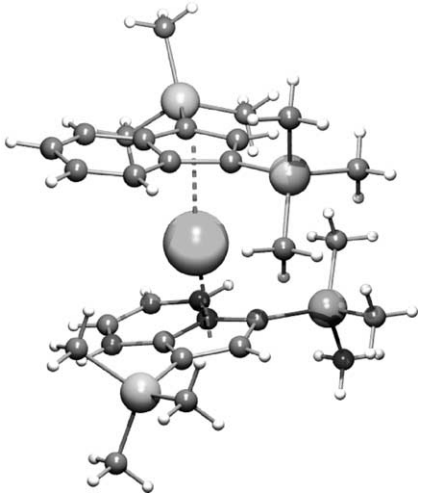

Fig. 3. The molecular structure of Pb{1,3-$(SiMe_3)_2$-Ind}$_2$ (NEBQUG).

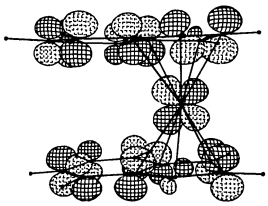

Scheme 6.

Since there are two rings and only one extra electron, this effect is still small, the folding angle being 7.3°, but ΔM–C is already 0.116 and 0.134 Å.

The same essentially holds for the Rh(II) derivative HAFDEX (Fig. 1), where small slip and folding parameters are found, together with an almost eclipsed ring (there is only one substituent in one of the rings).

In $NiInd_2$, the presence of a second electron in metal-ring antibonding orbitals induces larger folding (ca. 14°) and slippage (from 0.342 to 0.360 Å). Also, for electronic reasons, namely a better directionality of the metal orbitals, [2a] the staggered conformation of the rings becomes more stable and is indeed observed in all three examples (two independent molecules in TIBJOD, VILWAO; see Fig. 1). However, even in these complexes there is only one extra electron per ring in comparison with the 18 electron count. The indenyl coordination cannot yet be described as η^3, although it is no longer η^5: it is intermediate. Similar coordination modes have been described in detail [6n,6o].

The next group of complexes consists of electron deficient complexes, where the metal does not reach the 18 electron count. The first example is an analogue of the ferricium cation, $[Fe(1,3\text{-}Me_2\text{-}Ind)_2]^+$ (MINDFE). The η^5 coordination is still apparent, with ΔM–C values of ca. 0.075 Å and a folding angle of 4.4°. Indeed, the HOMO of ferrocene is only barely bonding (Scheme 7) and the removal of one electron does not lead to dramatic geometry changes. More interesting is the RA angle of 93.1°. Besides the steric effects which lead to a movement of the rings away from each other to avoid repulsion between the substituents in positions 1 and 3, there is a network of weak C–H···F hydrogen bonds between the anion and the cation [C–H···F 2.503 Å, 163.0°; C–H···F 2.542 Å, 153.8°, C–H···F 2.411 Å, 166.6° (1+x, y, 1+z); C–H···F 2.493 Å, 149.0° (1+x, y, z)] (Fig. 4).

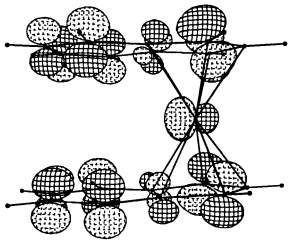

Scheme 7.

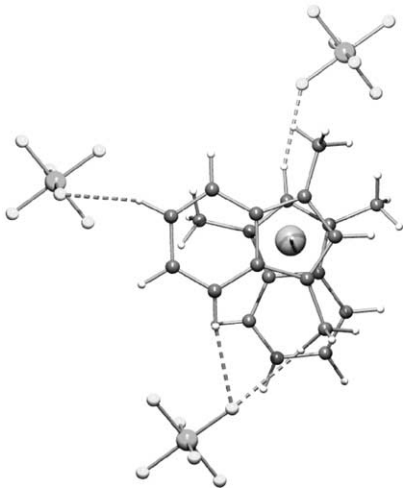

Fig. 4. The network of C–H···F hydrogen bonds in the crystal structure of $Fe\{1,3\text{-}Me_2\text{-}Ind\}_2$ (MINDFE).

The Cr(II) and Cr(III) complexes are only 16 and 15 electron species, respectively. Both molybdenum and tungsten behave differently, adding ligands to the $MInd_2$ unit in order to become electronically saturated (see later sections). The rings in the d^3 derivative $[CrInd_2^*]^+$ (YALPAC) can be considered η^5, as the folding is small (ca. 5°) and the slip is one of the smallest observed in this family of compounds (similar to that in $FeInd_2^*$). The M–C distances can be compared with those of $FeInd_2^*$ (VILWES) or $FeInd_2$ (DINDFE01), as both Cr and Fe are first row metals. They are longer, ranging between ca. 2.19 and 2.23 Å for Cr and between ca. 2.03 and 2.10 Å for Fe), a behavior which can be traced to the removal of electrons from metal-bonding levels in the Cr(III) derivative. This complex is paramagnetic with a quartet ground state [13].

There are two Cr(II) complexes (d^4). $CrInd_2^*$ (YALPEG) has been shown to have a triplet ground state, [13] with only two unpaired electrons, and is structurally close to $CoInd_2$ (VILVUH), both concerning slip (0.098) and folding (7.2°). The second species, $Cr\{1,3\text{-}(SiMe_3)_2\text{-}Ind\}_2$, is a high spin species with four unpaired electrons (not in the CCDC at the time of the search) [14]. The slip parameter is slightly larger (0.138Å), but both complexes are staggered (inversion center at the metal). The Cr–C distances are longer in the high spin species. DFT calculations (ADF program [15]) have been performed on a model $CrInd_2$, in order to understand the existence of the two forms. The energy difference is only 0.7 kcal mol^{-1}, the most stable species being the low spin one with two unpaired electrons. This small difference explains that it is easy to change from one to the other, a process, which may eventually be driven by the substituents. Indeed, while in the low spin form (YALPEG) the indenyl rings are permethylated, in the high

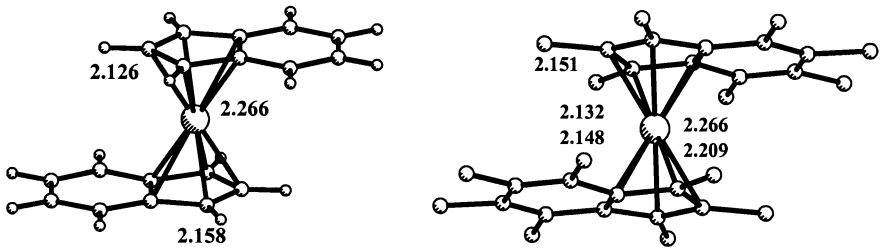

Scheme 8.

spin derivative there are two $SiMe_3$ substituents per ring. The more relevant distances are given for the low spin complex in Scheme 8 (calculated, left; X-ray, right; hydrogen atoms are not included).

The agreement between calculated and experimental distances is very good, considering that the substituents were not included in the calculations. The experimental distance Cr–C2 is longer than the calculated one, a fact, which may be due to the bulkiness of the methyl groups. The other distances are very similar and the spread is relatively small (ΔM–C 0.098 Å). The ring can be considered η^5-coordinated. The rings are staggered. Calculated and experimental Cr–C distances for the high spin complex are given in Scheme 9 (calculated, left; X-ray, right).

This species containing four unpaired electrons is different from the low spin one, but a good agreement between calculated and experimental distances was also obtained. All distances are in general longer than for the low spin form and the spread is larger. Indeed, there are two weak bonds to C4 and C9 (2.450 Å calculated; 2.398, 2.419 Å experimental). Although the calculations were performed on a model without any symmetry constraints, there is intrinsic symmetry in the molecule and equivalent distances are the same. The presence of 1,3 substituents in the real structure is a source of asymmetry and packing forces may also contribute to it. These long bonds are similar to those found in the Ni derivatives, so we can assume a similar coordination mode of the indenyl, namely between η^3 and η^5 (partial slippage).

Interestingly, the indenyl analogue of $CrInd_2^*$ could never be synthesized, the dimer $[CrInd_2]_2$ being observed in the solid state structure [16]. This suggests that the steric constraints introduced by the bulky Ind* or Ind′ ligands are needed to keep the metal center at this low electron count, the bulk of the substituents helping to tune the magnetic properties.

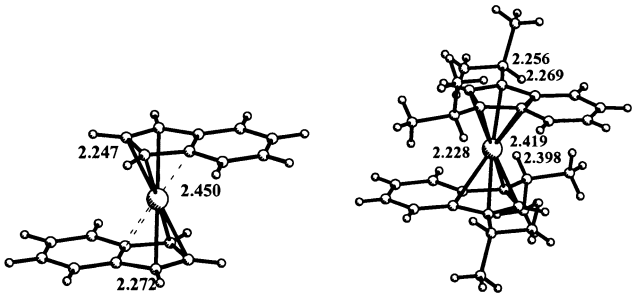

Scheme 9.

In this group of complexes there is a correlation between the degree of slippage, as reflected by the ΔM–C parameter, and the folding angle. While η^5 coordination is characterized by small values of ΔM–C and folding angles below 5°, as soon as the number of electrons increases and the M-ring antibonding orbital starts to be occupied, slippage starts in order to relieve that antibonding character and there is a concomitant increase in both parameters (1 electron, VILVUH, 0.12, 0.13 Å, 7.3°; two electrons, VILWAO, 0.42 Å, 13.6°). A similar reasoning can be applied, in principle, when the electron count falls below 18, although the paramagnetism of the complexes may complicate the interpretation. The Pb complex is the most striking deviation to any of these ideas, since the steric effects of the ring substituents can easily overcome the preference for η^1 coordination.

3.3. $MInd_2L_2$ compounds

The structural data concerning $MInd_2L_2$ complexes are collected in Table 3 together with CCDC refcodes. They are organized in groups according to the electron count, starting from 16 electron species. Structures of some representative complexes bearing two η^5-indenyl rings are given in Fig. 5. The substituted indenyl rings not shown in other figures are given in Scheme 10.

In the family of bent bis(indenyl)metal complexes, in addition to the torsion angle TA introduced above, another structural parameter needs to be considered, namely the orientation of the two indenyl ligands relative to the L–Mo–L′ plane, measured here as the rotation angle OA. It is defined as the angle that the projection of the vector, determined by the centroids of the five and the six membered rings on the LML′ plane, makes with the z line (Scheme 11). This z line is given by the intersection of the LML′ plane with the plane defined by the metal center and by the centroids of the five member rings of the two indenyl ligands. The difference |TA − OA| gives automatically the orientation

Table 3
Structural data for $MInd_2L_2$ complexes (distances in Å, angles in °)

Complex	Refcode	HA	HA′	ΔM–C	ΔM–C′	TA	OA	OA′	RA
[ZrInd′Ind″Br_2]	CEGQUA	7.5	4.6	0.085	0.086	34.4	105.7	67.3	61.4
[$TiInd_2$(NCPh)(NCMePh)]$^+$	GAXRIG	4.8	5.9	0.150	0.115	100.2	23.0	52.6	70.2
[$HfInd_2(Me)_2$]	INDMHF	5.6	5.6	0.109	0.109	62.5	28.7	28.7	52.0
[$TiInd_2(Me)_2$]	INDMTI	2.8	2.8	0.117	0.117	65.3	29.6	29.6	54.2
[$ZrInd_2(Me)_2$]	INDMZR	4.9	4.9	0.103	0.103	61.8	28.3	28.3	51.6
[$ZrInd'_2(CH_2Ph)_2$]	JIGZOO	4.8	4.4	0.125	0.079	110.5	29.9	146.0	122.7
[$ZrInd'_2Cl_2$]	LAWYOX	11.8	9.3	0.061	0.064	71.1	106.5	30.5	85.8
	LAWYOX	8.3	8.5	0.069	0.075	79.6	35.6	38.7	65.1
[$ZrInd'_2Cl_2$]	LOCMEV	4.6	4.0	0.071	0.125	95.5	62.4	17.8	74.3
[$ZrInd'_2Cl_2$]	NAGJEK	12.3	13.7	0.054	0.045	126.1	64.2	54.0	104.3
	NAGJEK	13.7	14.8	0.067	0.046	121.0	60.8	52.2	100.3
[$TaInd_2Cl_2$]$^+$	NAZBEV	6.3	6.4	0.138	0.132	50.5	34.0	93.8	115.4
[$ZrInd'_2Cl_2$]	NEVVUF	8.8	8.6	0.061	0.075	147.5	72.6	109.1	60.4
[$ZrInd'_2Cl_2$]	NEVWAM	2.7	7.9	0.027	0.056	30.2	72.0	105.3	56.7
[$HfInd'_2Cl_2$]	NISFOK	2.6	8.0	0.100	0.114	32.6	109.0	72.3	60.3
	NISFOK	5.6	5.4	0.050	0.072	171.5	90.3	99.4	48.0
	NISFOK01	5.5	5.6	0.055	0.067	171.6	89.8	99.1	48.6
	NISFOK01	7.7	3.4	0.081	0.089	33.5	71.3	109.2	61.0
	NUWFOA	4.8	8.2	0.040	0.017	127.9	72.2	129.7	75.1
[$(YInd'_2)_2(\mu\text{-}H)_2$]	PURDIP	3.2	3.3	0.025	0.038	163.8	76.5	94.9	50.8
	PURDIP	3.9	3.4	0.055	0.022	161.8	92.3	108.1	128.4
[$ZrInd'_2Cl_2$]	QAHHUC	3.0	3.5	0.092	0.099	51.8	21.5	24.9	42.2
[$ZrInd'_2Cl_2$]	QAHJAK	3.9	3.9	0.081	0.081	175.9	87.1	92.9	48.7
[$ZrInd_2Cl_2$]	RIFPAX	5.2	6.2	0.108	0.115	45.9	22.8	18.1	36.3
[$ZrInd'_2Cl_2$]	TOMFIK	12.5	12.8	0.059	0.047	126.6	59.2	120.3	75.5
	TOMFIK01	12.5	12.5	0.054	0.054	126.7	59.6	120.4	75.5
[$ZrInd'_2Cl_2$]	YAPZIY	4.0	4.0	0.060	0.060	57.5	26.1	26.1	47.3
[$ZrInd'_2Cl_2$]	YAPZOE	1.7	3.0	0.093	0.066	176.6	39.1	44.0	32.7
[$ZrInd'_2Cl_2$]	YEXNOE	5.7	5.2	0.052	0.060	171.2	89.6	99.7	49.0
	YEXNOE	3.8	6.4	0.097	0.068	33.0	109.0	71.8	60.7
	YEXNOE01	6.1	5.3	0.105	0.068	32.2	108.8	72.8	60.5
	YEXNOE01	4.8	6.3	0.065	0.053	171.0	99.8	89.8	49.2
	YEXNOE02	5.7	5.2	0.052	0.060	171.2	89.6	99.7	49.0
	YEXNOE02	3.8	6.4	0.097	0.068	33.0	109.0	71.8	60.7
[$ZrInd^*_2Cl_2$]	YIGDOH	6.4	5.9	0.051	0.047	101.1	53.4	43.4	88.9
[$ZrInd'_2Cl_2$]	ZILWOG	8.7	3.5	0.070	0.084	31.6	105.8	69.8	61.3
[$ZrInd'_2Cl_2$]	ZILWUM	5.6	6.2	0.062	0.043	123.9	72.1	133.0	75.7
[$YbInd_2${$MeO(CH_2)_2OMe$}]	HOTPOV	4.5	4.5	0.053	0.053	39.9	18.0	18.0	31.6
[$ErInd_2Cl(THF)$]	MAQHOB	4.8	4.3	0.044	0.045	34.0	36.5	108.3	128.1
[$YbInd'_2\{\kappa_2\text{-}Cl_2Li(THF)\}_2$]	MAQHUH	1.1	3.4	0.087	0.062	177.5	37.7	138.4	148.8
[$HfInd_2Cl_2$]	PEKKOF	1.5	3.8	0.043	0.024	171.1	94.6	85.3	52.2
	PEKKOF01	1.1	1.1	0.035	0.035	171.1	94.6	85.4	52.1
[$\{SmInd_2(THF)\}_2(\mu\text{-}O)$]	RABTOZ	1.7	3.2	0.063	0.089	107.9	35.0	69.5	92.5
	RABTOZ	1.7	3.2	0.063	0.089	107.9	35.0	69.5	92.5
[$UInd_2(BH_4)_2$]	VASVUG	6.1	9.0	0.006	0.066	136.0	38.4	87.0	69.8
[$MoInd_2(\kappa_2\text{-}S_2CNEt_2)$]$^+$	BAMHOM	4.1	3.3	0.124	0.169	9.4	82.2	93.3	46.0
[$MoInd_2(\kappa_2\text{-}S_2CNEt_2)$]$^+$	BAMHOM	4.0	5.4	0.147	0.148	0.9	83.8	82.7	43.6
[$MoInd(\eta^3\text{-}Ind)\{P(OMe)_3\}_2$]$^{2+}$	[17]	3.5	6.1	0.135	0.181	95.5	3.5	85.8	83.2
[$MoInd(\eta^3\text{-}Ind)(CO)Cl$]$^+$	[17]	5.4	5.5	0.158	0.169	5.9	83.0	89.1	44.6
[$MoInd(\eta^3\text{-}Ind)(CO)Br$]$^+$	[17]	7.2	6.3	0.156	0.157	3.3	88.8	89.1	44.9
[$MoInd(\eta^3\text{-}Ind)Br_2$]	[17]	6.6	3.6	0.159	0.171	177.0	87.3	88.8	46.5
		6.4	5.2	0.157	0.195	176.3	87.3	86.7	46.1
		3.8	5.9	0.165	0.199	12.1	86.2	80.6	47.2
		2.4	5.1	0.180	0.168	15.4	78.0	84.2	49.6
[$VInd_2(CO)_2$]	FIVXOX	6.3	4.7	0.130	0.142	5.7	76.4	82.9	41.6
[$TiInd_2(CO_2)$]	GIRZUC	3.7	3.8	0.097	0.135	16.4	77.2	84.9	137.7
	GIRZUC	4.1	2.9	0.092	0.103	176.4	96.3	94.4	39.3
[$ZrInd_2(CO_2)$]	GISBAL	3.9	3.2	0.101	0.087	3.6	97.5	93.8	34.9

Table 3 (*Continued*)

Complex	Refcode	HA	HA′	ΔM–C	ΔM–C′	TA	OA	OA′	RA
[Ind(η^3-Ind)V(CO)$_2$]	DOPTIL	4.4	12.0	0.122	0.498	179.7	5.7	5.4	3.4
[MoInd(η^3-Ind)(CO)$_2$]	BAMGUR	20.9	3.0	0.721	0.115	179.8	3.8	4.2	2.3
[Ind(η^3-Ind)Mo(dppe)]	WAJWOT	25.6	3.7	0.717	0.133	89.9	0.9	92.1	92.2
[WInd(η^3-Ind)(CO)$_2$]	[18]	25.6	1.2	0.764	0.079	179.3	4.5	5.4	176.6

of the second indenyl ligand. However, if this expression is used, the values for the second indenyls are slightly different from those in Table 3. This small discrepancy is due to the fact in the X-ray structure the line defined by the centroid of the C_5 ring and the metal center intersects the indenyl ring at near 90°.

The largest family in this group of compounds consists of d^0 transition metal derivatives, some of them having a partly filled f shell. Most of them are Zr(IV) chloro or methyl complexes, with indenyl rings bearing a wide variety of substituents, from the point of view of both their electronic and steric properties. Before further discussion, it is instructive to observe the correlation curve ΔM–C versus folding angle Ω (Fig. 6).

There is essentially no correlation except for the four points with larger slippage (to which we shall return later), in agreement with the idea given by the values in Table 3. Except for those four complexes, all are formally 16–18 electron species and it is expected that the indenyl is planar and η^5-coordinated. In the group of 16 electron species, ΔM–C values are not much spread (< 0.12 Å), but the folding angles can be as high as 14.8° in the Zr complex NAGJEK (Fig. 5). In this compound the *N*-pyrrolidinyl substituent at the 2 position of the indenyl forces the folding of the indenyl, in order to relieve repulsion. The ΔM–C parameter always indicates η^5 coordination, but the rings are often far from planar. Also, the TA angles can vary over a wide range of values, from ca. 30 to 178°. Only eclipsed rings are prevented by strong repulsions between adjacent indenyl rings. Steric effects are responsible for these spreads.

DFT calculations [8] (ADF program [15]) were performed on several $MInd_2L_2$ complexes, the L ligand chosen being CO, since there are examples of CO derivatives for almost all electron counts. For the 16 electron species, the model is $[ZrInd_2(CO)_2]^{2+}$. The calculated Zr–C distances range from 2.478 to 2.580 Å, the '3 shorter+2 longer' bond pattern being usually observed, and agree very well in general with the typical distances found for the available sample. Considering that many of the indenyl ligands bear bulky substituents, deviations arising from substituent effects are expected. The calculated rotation angle RA is 70.4°, while TA is 124.3°, OA1 63.1°, and OA2 56.9°, which again fit the distribution of experimental values.

The family of 18 electron bis(indenyl)ML_2 derivatives consists of five Mo(IV) complexes, dicationic, monocationic and neutral, as well as the carbonyl derivatives of Ti, Zr and $[VInd_2(CO)_2]^+$. The distances calculated (Scheme 12, left) for $[ZrInd_2(CO)_2]^{2+}$ agree very well with the experimental ones (GISBAL; Scheme 12, right). Owing to the asymmetry of the indenyl rings, the two Zr–C(CO) bonds are rather different (calc. 2.20, 2.19 Å; exp. 2.22, 2.18 Å). The same asymmetry is noticed in the Zr–C(Ind) bonds, and as a result the Zr–C(2) bond is sometimes slightly longer than Zr–C(1). However, the two bonds to C(4) and C(9) remain the longest (calc. 2.60–2.62 Å; exp. 2.55, 2.59 Å).

In the case of the molybdenum derivatives, the calculated distances could only be compared with those of $[MoInd_2(CO)X]^+$ (X = Cl, Br), [18] since the dicarbonyl cation has not been structurally characterized. When X = Cl, the Mo–C(CO) distances are 1.99 (exp.) and 2.04 Å (calc.), while the Mo–C(Ind) bonds follow the same pattern as in the Zr derivative, the shortest one being Mo–C(1), and the longest those to C(4) and C(9).

The conformations of the indenyl rings are different in the calculated and X-ray structures. There was no attempt to find the absolute minimum, especially because even for the same compound, several arrangements are found sometimes in the unit cell. An example is provided by $[HfInd_2Cl_2]$ (NISFOK), for which the two TA angles differ as much as 32.6 and 171.5°, and there are others, such as $[Zr(2\text{-Ph–Ind})_2Cl_2]$ (YEXNOE). Two of the possible conformations found in the X-ray structure are given in Fig. 7.

In order to explore this aspect, molecular mechanics calculations [19] (carried out using the universal force field within CERIUS2 [20]) were performed for some complexes, using an approach similar to the one described previously [21]. Some results are given in Table 4 for two Zr complexes, with an indenyl ring and a heptamethylindenyl one.

These results suggest that when the ring has no substituents, there are many different conformations with very similar energies (within 2.4 kcal mol^{-1} in GISBAL). The introduction of substituents, as expected, favors some conformations relative to others. For the Ind* complex, the energy differences go up to more than 20 kcal mol^{-1}. Therefore, the coexistence of several indenyl arrangements should not occur when there are bulky substituents on the ring.

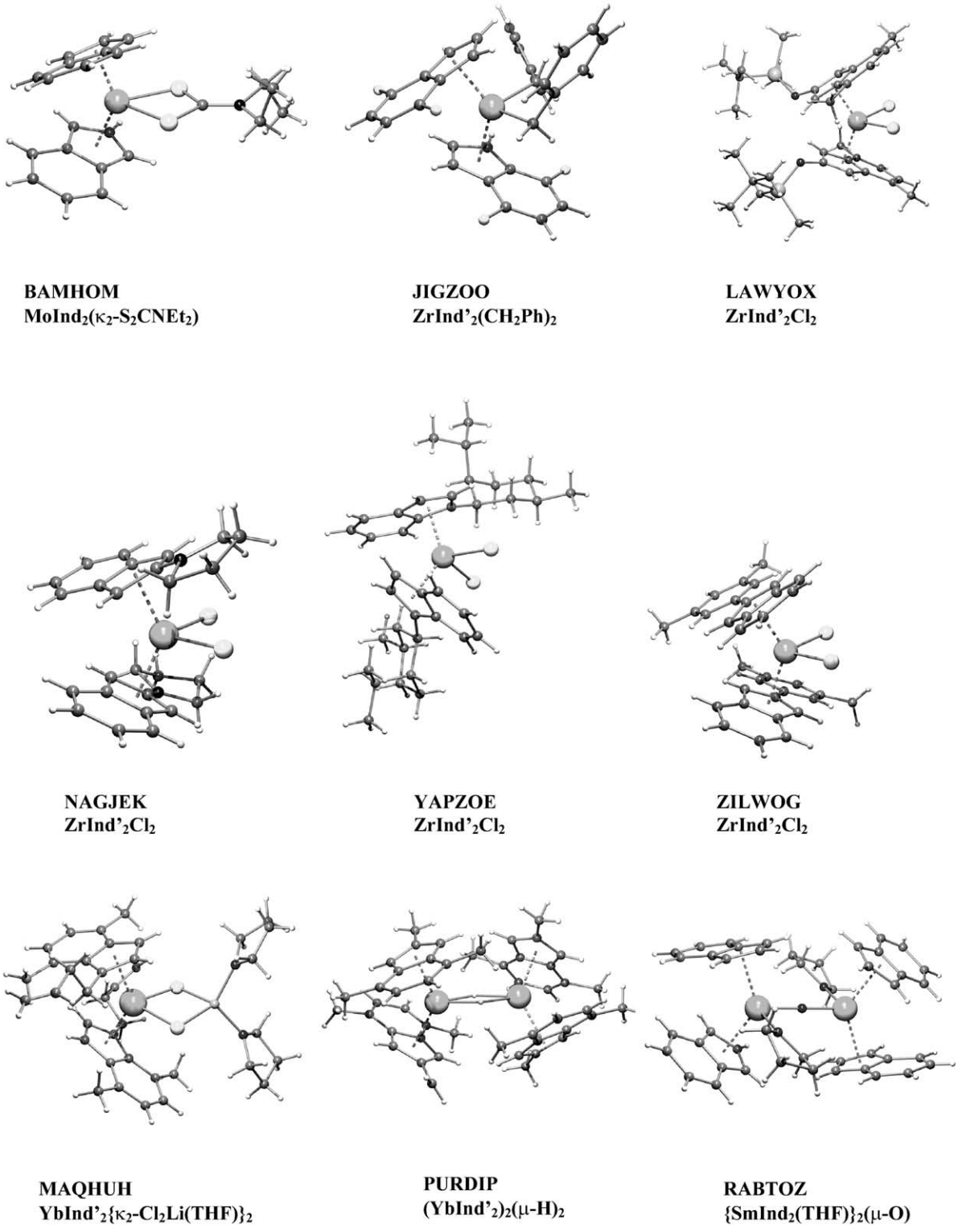

Fig. 5. Molecular structures of some relevant $M(\eta^5\text{-}Ind_2)L_2$ complexes featuring indenyl rings with bulky substituents, mononuclear (BAMHOM, JIGZOO, LAWYOX, NAGJEK, YAPZOY, ZILWOG) and binuclear (MAQHUH, PURDIP, RABTOZ).

The remaining four complexes in Table 3 (Fig. 8) have a formal electron count higher than 18, and both ΔM–C and the folding angle relative to one ring are very different from the other, indicating that ring slippage is taking place. These compounds correspond to the four points at the right side of Fig. 6.

In the η^3-indenyl rings of $MInd_2L_2$ complexes it is better to change slightly the definitions given earlier for

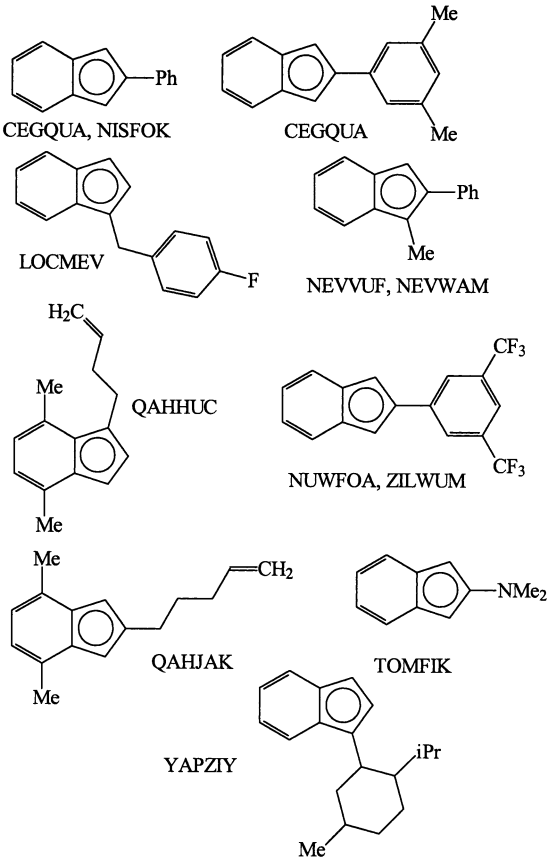

Scheme 10.

TA and OA, using the midpoint of the two carbon atoms adjacent to the six member ring (atoms C(1) and C(3) in Scheme 1), instead of the centroid of the five member ring.

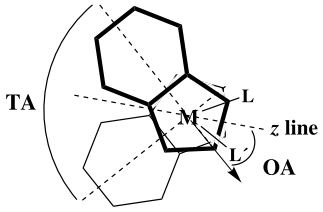

Scheme 11.

The first complex, $[VInd_2(CO)_2]$ (DOPTIL, Fig. 8) can be compared with its cationic analogue. The addition of one electron has as main result the weakening of two V–C(4) and V–C(9) bonds in one of the indenyl rings (2.88, 2.86 Å), compared with the same bonds in the second ring (2.39 Å) and in the neutral compound (2.36, 2.41 Å and 2.38, 2.40 Å, respectively in each ring). These longer distances are very similar to those calculated (ADF program) for the paramagnetic species $[MoInd_2\{P(OH)_3\}_2]^+$, which has the same electron count [6o]. They also follow the same trend as the Ni–C distances in $[NiInd_2]$ where one electron in average is added to each ring and distances also increase by comparable amounts, as referred above. The folding angles are also almost the same in these examples (ca. 12–14°). The two molybdenum compounds (BAMGUR and WAJWOT), as well as $[WInd_2(CO)_2]$ [18] are formally 20 electron compounds. As a result, the slippage is more pronounced, with the Mo distances to C(4) and C(9) in BAMGUR 3.14 and 3.17 Å, and the

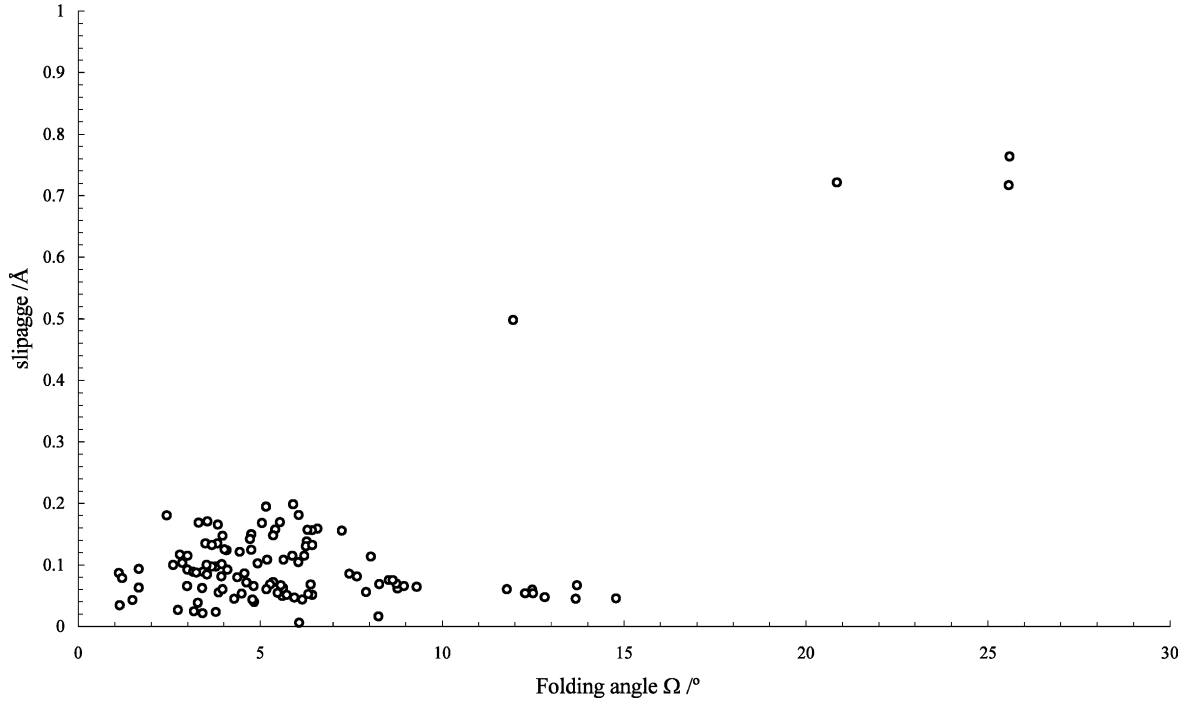

Fig. 6. Statistical correlation between slippage parameters (ΔM–C) and folding angles (Ω).

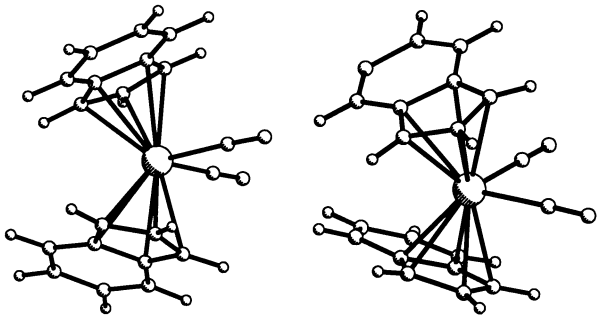

Scheme 12.

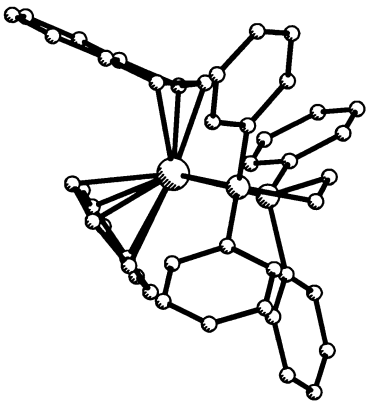

Scheme 13.

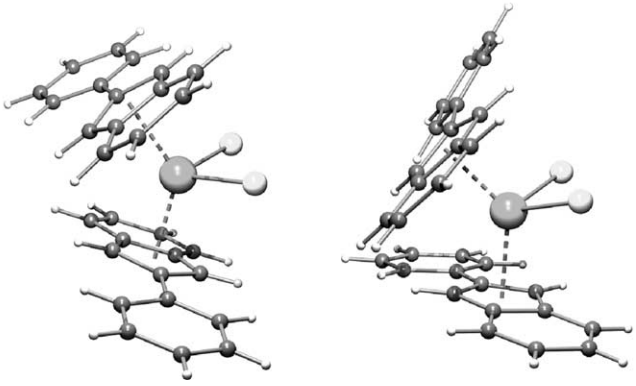

Fig. 7. Two different arrangements of the indenyl rings in the X-ray structure of [Zr(2-Ph–Ind)$_2$Cl$_2$] (YEXNOE).

folding angle 20.9°. Still larger foldings are observed for the other two examples (25.6 and 25.5°). The structures shown in Fig. 8 belong to the same type, with TA angles very close to 180°, but with orientation angles close to 0°. This indicates that the two carbonyl ligands lie under the benzene ring of the indenyl ligand, an arrangement which has not been found in the M(η^5-Ind)$_2$L$_2$ species and is favored by electronic reasons because back-donation to the carbonyls is enhanced [6k].

The other complex in this family, WAJWOT, deviates from this pattern since the rings are not staggered (TA 89.9°) and the OA angles are, respectively 0.9 and 92.1°, much closer to the M(η^5-Ind)$_2$L$_2$ complexes. The explanation resides in the steric effect of the four phenyl groups of dppe, which prevents the indenyl to lie over the L ligands, and forces them to move away (Scheme 13).

In these complexes, contrary to what happened in MInd$_2$, the addition of two electrons causes one indenyl ring to change from η^5 to η^3, while the same effect in NiInd$_2$ results in an intermediate slippage and folding of both rings.

A qualitative explanation can be given based on extended Hückel calculations [22] (CACAO program [23]). Calculations were performed on model complexes [MoInd$_2$(CO)$_2$] and [MoInd$_2$(PH$_3$)$_2$], with the two indenyl rings in limiting conformations. The HOMOs of the four species are shown in Fig. 9.

The HOMOs of the carbonyl complexes are different, because when the rings are staggered (left) the orbital is much more localized in the Mo and the carbonyls. The eclipsed conformation of the rings leads to more delocalized orbitals, with also strong contributions from the ring. These orbitals are Mo-ring antibonding, reminding of the representation on Scheme 6, but also Mo–CO bonding (backdonation). The stronger locali-

Table 4
The calculated relative energies (molecular mechanics) of chosen conformations of [ZrInd$_2$(CO)$_2$] (GISBAL) and [ZrInd$_2^*$Cl$_2$] (YIGDOH) (angles in °)

Complex	Refcode	OA1	OA2	TA	ΔE (kcal mol^{-1})
[ZrInd$_2$(CO)$_2$]	GISBAL	90	0	90.8	1.9
		90	−180	89.3	1.4
		180	−180	0	0.9
		0	−180	180	2.4
		90	90	179.3	0.0
[ZrInd$_2^*$Cl$_2$]	YIGDOH	0	90	91.0	0.0
		180	90	88.9	15.6
		0	180	2.4	18.3
		90	−90	1.5	21.5
		90	90	178.6	2.1

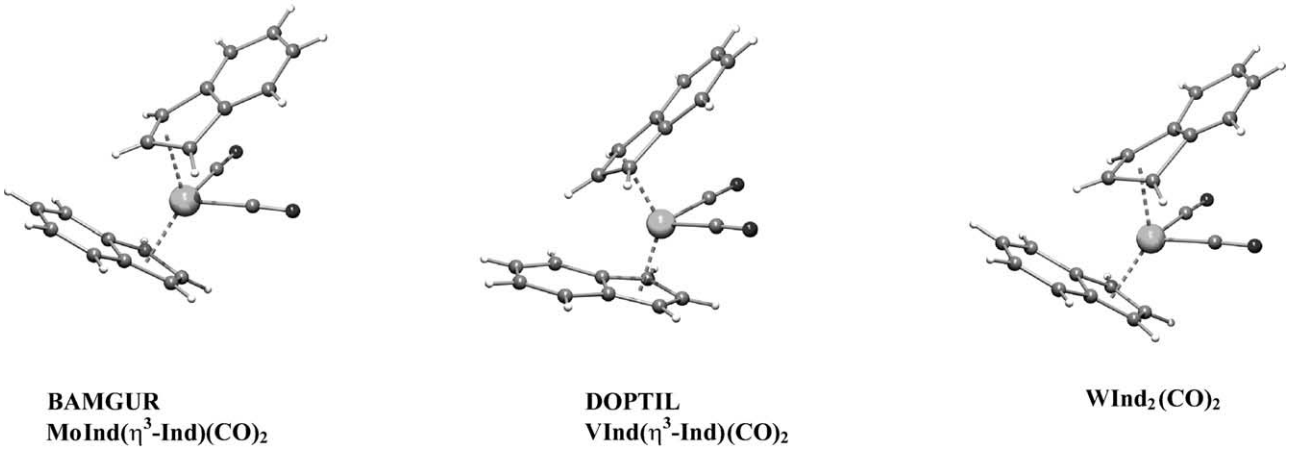

Fig. 8. Molecular structures of $M(\eta^5\text{-Ind})(\eta^3\text{-Ind})L_2$ complexes (BAMGUR, DOPTIL, $[WInd_2(CO)_2]$).

Table 5
Structural data for $MInd_2L_n$ ($n = 1, 3$) complexes (distances in Å, angles in °)

	Refcode	HA	HA′	ΔM–C	ΔM–C′	TA	OA1	OA2	RA
$[VInd_2I]$	FIVXIR	0.3	0.3	0.071		−6.4	80.7	73.6	37.4
$[(PrInd_2THF)_2(\mu\text{-}Cl)_2]$	GAQMIU	9.5	6.1	0.101	0.078	−177.2	10.7	13.2	11.9
$[(SmInd_2)(THF)_3]$	PIRYUK	8.6	8.6	0.023	0.023	−38.3	17.0	17.0	29.2

zation of the HOMO in this fragment leads to a further stabilization (increased backdonation and less Mo-ring antibonding character), reflected in a lower energy (0.22 eV, 5 kcal mol^{-1}). There is therefore a marked electronic preference in the carbonyl derivatives and the staggered arrangement is observed in all the examples given in Fig. 8. Let us now consider the phosphine complexes. The composition and energy of the HOMOs in the lower part of Fig. 9 are almost independent of the conformation of the ring. There is not a relevant electronic preference. On the other hand, phosphines usually carry bulky substituents, favoring the eclipsed conformation of the rings. This is reflected in Scheme 13, where dppe (1,2-diphenylphosphine methane) is coordinated to Mo and the rings adopt an intermediate conformation.

The relative conformation of the two Ind ligands in $[(Ind)_2ML_2]$ complexes, as a function of the metal M, and the ligands L, is currently being studied in more detail using DFT methods, and will be the subject of a forthcoming publication.

3.4. $MInd_2L_n$ ($n = 1, 3$) compounds

The structural data concerning $MInd_2L_n$ ($n = 1, 3$) complexes are collected in Table 5 together with CCDC refcodes. Structures of the three available complexes are given in Fig. 10.

The indenyl rings have no substituents, the ΔM–C values are within 0.1 Å and the folding angles are relatively small (between 0.3° in the V derivative and a maximum of 9.5° in GAQMIU). Therefore, the rings can be considered η^5-coordinate.

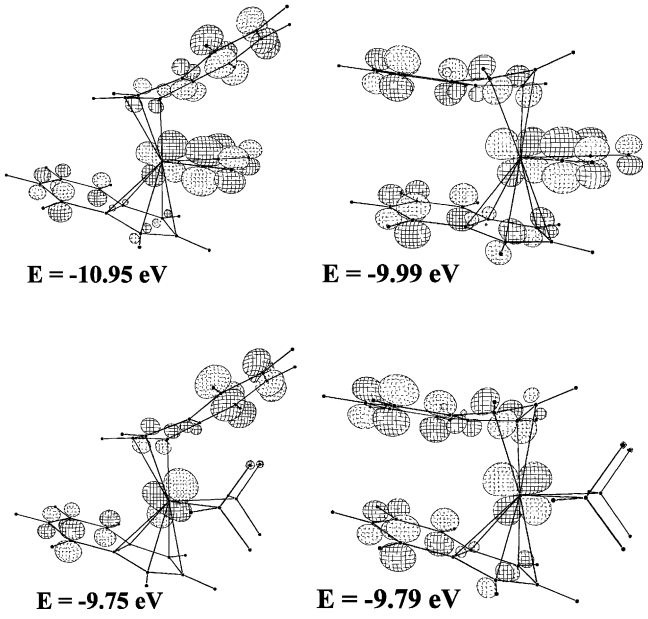

Fig. 9. The HOMOs of $[MoInd_2(CO)_2]^{2+}$ (top) and $[MoInd_2(PH_3)_2]^{2+}$ (bottom) for two limiting conformations of the benzene rings.

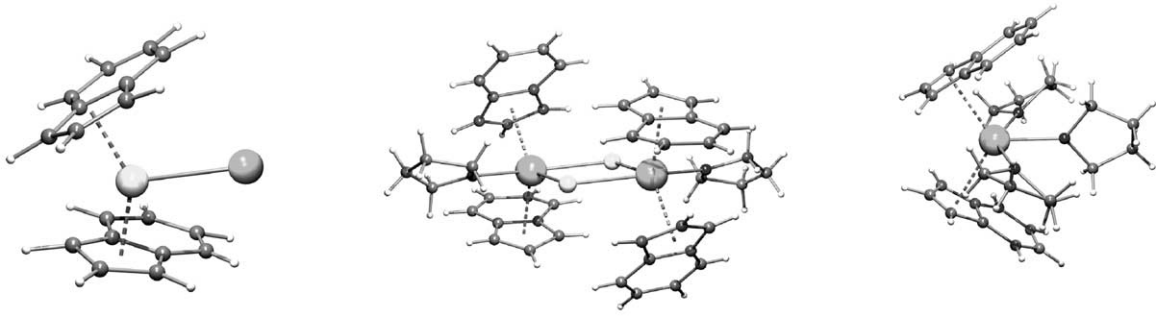

Fig. 10. Molecular structures of $M(Ind_2)L_n$ complexes (FIVXIR, GAQMIU, PIRYUK).

4. Conclusions

In all the groups of complexes analyzed, the rotation angles between the indenyl rings vary considerably. For $MInd_2$ complexes the rings prefer to be eclipsed in 18 electron species and staggered as the electron count increases and the ring starts to slip. The presence of bulky substituents in the rings may reverse this picture. In the family of $MInd_2L_2$ complexes, although for 16–18 electron counts the rings should be coordinated in a η^5 mode, in many Zr derivatives folding angles up to 14° can be observed. Usually, there is a sterical repulsion in such cases. The electronic driving force (decrease of antibonding character when metal-ring antibonding orbitals are occupied) for folding is accompanied by a large folding, not seen in the previous cases, and its magnitude is proportional to the number of excess electrons, as shown for the available cases. Finally, it is interesting to notice that while in $NiInd_2$ the addition of two electrons causes both rings to slip and fold by intermediate amounts, in $MoInd_2L_2$ species only one ring slips and becomes η^3.

5. Computational details

Density functional calculations [8] were carried out with the Amsterdam Density Functional (ADF2.3 and 2000) program developed by Baerends and coworkers [15]. Vosko, Wilk and Nusair's local exchange correlation potential was used [24]. Gradient corrected geometry optimizations [25] were performed using the generalized gradient approximation (Becke's exchange [26] and Perdew's [27] correlation functionals). Unrestricted calculations were performed for all the paramagnetic species studied. The core orbitals were frozen for Mo ([1–3]s, [1–3]p, 3d) and C, N, O (1s). Triple ζ Slater-type orbitals (STO) were used for H 1s, C, O 2s and 2p, Mo 4s and 4p. A set of polarization functions was added: H (single ζ, 2p), C, N, O (single ζ, 3d). Full geometry optimizations were performed without any symmetry constraints on models based on the available crystal structures, as described in the text.

Ab initio and DFT calculations were also performed with the GAUSSIAN-98 program [11]. The B3LYP hybrid functional with a standard LanL2DZ basis set [28], was used in all calculations. That functional includes a mixture of Hartree-Fock [29] exchange with DFT [8] exchange-correlation, given by Becke's three parameter functional [30] with the Lee, Yang and Parr correlation functional, which includes both local and non-local terms [31]. Fully optimized geometries were obtained without any symmetry constraints.

The extended Hückel calculations [22] were done with the CACAO program [23] and modified H_{ij} values were used [32]. The basis set for the metal atoms consisted of ns, np and $(n-1)$d orbitals. The s and p orbitals were described by single Slater-type wave functions, and the d orbitals were taken as contracted linear combinations of two Slater-type wave functions. The parameters used for Mo were the following (H_{ii} (eV), ζ): 5s —8.77, 1.960; 5p —5.60, 1.900; 4d —11.06, 4.542, 1.901 (ζ_2), 0.5899 (C_1), 0.5899 (C_2). Standard parameters were used for other atoms. Calculations were performed on models based on the optimized geometries with idealized maximum symmetry, and the following distances (Å): M–(C_5 ring centroid) 2.00, M–C(CO) 2.00, C–O 1.15, C–C 1.40, C–H 1.08; and a folding angle $\Omega = 30°$.

Acknowledgements

POCTI/36127/QUIM/2000 is acknowledged for partial funding of this work.

References

[1] M.E. Rerek, L.-N. Ji, F. Basolo, J. Chem. Soc. Chem. Commun. (1983) 1208.

[2] (a) M.J. Calhorda, L.F. Veiros, J. Organomet. Chem. 635 (2001) 197;
(b) S.A. Westcott, A.K. Kakkar, G. Stringer, N.J. Taylor, T.B. Marder, J. Organomet. Chem. 394 (1990) 777.
[3] L. Resconi, L. Cavallo, A. Fait, F. Piemontesi, Chem. Rev. 100 (2000) 1253.
[4] (a) M. Linnolahti, P. Hirva, J. Comput. Chem. 22 (2001) 51;
(b) M. Linnolahti, T.A. Pakkanen, R. Leino, H.J.G. Luttikhedde, C.-E. Wilén, J.H. Näsman, Eur. J. Inorg. Chem. (2001) 2033;
(c) M. Linnolahti, T.A. Pakkanen, Macromolecules 33 (2000) 9205;
(d) N. Mäkelä, H.R. Kuutila, M. Linnolahti, T.A. Pakkanen, J. Chem. Soc. Dalton Trans. (2001) 91.
[5] (a) L.-N. Ji, M.E. Rerek, F. Basolo, Organometallics 3 (1984) 740;
(b) W. Simanko, V.N. Sapunov, R. Schmid, K. Kirchner, S. Wherland, Organometallics 17 (1998) 2391;
(c) E.U. Van Raaij, H.H. Brintzinger, L. Zsolnai, G. Huttner, Z. Anorg. Allg. Chem. 577 (1989) 217;
(d) R.M. Kowalewski, A.L. Rheingold, W.C. Trogler, F. Basolo, J. Am. Chem. Soc. 108 (1986) 2460;
(e) Z. Zhou, C. Jablonski, J. Brisdon, J. Organomet. Chem. 461 (1993) 215;
(f) D.A. Brown, N.J. Fitzpatrick, W.K. Glass, H.A. Ahmed, D. Cunningham, P. McArdle, J. Organomet. Chem. 455 (1993) 157;
(g) K.A. Pevear, M.M. Banaszak Holl, G.B. Carpenter, A.L. Rieger, P.H. Rieger, D.A. Sweigart, Organometallics 14 (1995) 512;
(h) J.S. Merola, R.T. Kacmarcik, D. Van Engen, J. Am. Chem. Soc. 108 (1986) 329;
(i) R. Poli, S.P. Mattamana, L.R. Falvello, Gazz. Chim. Ital. 122 (1992) 315;
(j) J.R. Ascenso, C.G. Azevedo, I.S. Gonçalves, E. Herdtweck, D.S. Moreno, C.C. Romão, J. Zühlke, Organometallics 13 (1994) 429;
(k) I.S. Gonçalves, C.C. Romão, J. Organomet. Chem. 486 (1995) 155;
(l) J.W. Faller, R.H. Crabtree, A. Habib, Organometallics 4 (1985) 929;
(m) T.A. Huber, M. Bayrakdarian, S. Dion, I. Dubuc, F. Bélanger-Gariépy, D. Zargarian, Organometallics 16 (1997) 5811;
(n) R.H. Crabtree, C.P. Panell, Organometallics 3 (1984) 1727;
(o) T.B. Marder, J.C. Calabrese, D.C. Roe, T.H. Tulip, Organometallics 6 (1987) 2012;
(p) A. Georg, C.G. Kreiter, Eur. J. Inorg. Chem. (1999) 651;
(q) G.J. Kubas, G. Kiss, C.D. Hoff, Organometallics 10 (1991) 2870;
(r) R.N. Biagioni, I.M. Lorkovic, J. Skelton, J.B. Hartung, Organometallics 9 (1990) 547;
(s) A. Decken, S.S. Rigby, L. Girard, A.D. Bain, M.J. McGlinchey, Organometallics 16 (1997) 1308;
(t) G.M. Diamond, M.L.H. Green, P. Mountford, N.A. Popham, A.N. Chernega, J. Chem. Soc. Chem. Commun. (1994) 103;
(u) M. Bochmann, S.J. Lancaster, M.B. Hursthouse, M. Mazid, Organometallics 12 (1993) 4718;
(v) R.T. Baker, T.H. Tulip, Organometallics 5 (1986) 839;
(x) F.H. Köhler, Chem. Ber. 107 (1974) 570.
[6] (a) A. Decken, J.F. Britten, M.J. McGlinchey, J. Am. Chem. Soc. 115 (1993) 7275;
(b) A. Decken, S.S. Rigby, L. Girard, A.D. Bain, M.J. McGlinchey, Organometallics 16 (1997) 1308;
(c) T.A. Albright, P. Hofmann, R. Hoffmann, C.P. Lillya, P.A. Dobosh, J. Am. Chem. Soc. 105 (1983) 3396;
(d) A.K. Kakkar, N.J. Taylor, J.C. Calabrese, W.A. Nugent, D.C. Roe, E.A. Connaway, T.B. Marder, J. Chem. Soc. Chem. Commun. (1989) 990;
(e) N.S. Crossley, J.C. Green, A. Nagy, G. Stringer, J. Chem. Soc. Dalton Trans. (1989) 2139;
(f) T.M. Frankcom, J.C. Green, A. Nagy, A.K. Kakkar, T.B. Marder, Organometallics 12 (1993) 3688;
(g) J.C. Green, R.P.G. Parkin, X. Yang, A. Haaland, W. Scherer, M. Tapifolsky, J. Chem. Soc. Dalton Trans. (1997) 3219;
(h) C.N. Field, J.C. Green, A.G.J. Moody, M.R.F. Siggel, Chem. Phys. 206 (1996) 211;
(i) C. Bonifaci, A. Ceccon, S. Santi, C. Mealli, R. Zoellner, R.W. Inorg. Chim. Acta 240 (1995) 541;
(j) M.J. Calhorda, L.F. Veiros, Coord. Chem. Rev. 185–186 (1999) 37;
(k) M.J. Calhorda, C.A. Gamelas, I.S. Gonçalves, E. Herdtweck, C.C. Romão, L.F. Veiros, Organometallics 17 (1998) 2597;
(l) M.J. Calhorda, C.A. Gamelas, C.C. Romão, L.F. Veiros, Eur. J. Inorg. Chem. (2000) 331;
(m) L.F. Veiros, J. Organomet. Chem. 587 (1999) 221;
(n) L.F. Veiros, Organometallics 19 (2000) 3127;
(o) M.E. Stoll, P. Belanzoni, M.J. Calhorda, M.G.B. Drew, V. Félix, W.E. Geiger, C.A. Gamelas, I.S. Gonçalves, C.C. Romão, L.F. Veiros, J. Am. Chem. Soc. 123 (2001) 10595.
[7] F.H. Allen, J.E. Davies, J.J. Galloy, O. Johnson, O. Kennard, C.F. Macrae, E.M. Mitchell, G.F. Mitchel, J.M. Smith, D.G. Watson, J. Chem. Inf. Comput. Sci. 31 (1991) 187.
[8] R.G. Parr, W. Yang, Density Functional Theory of Atoms and Molecules, Oxford University Press, New York, 1989.
[9] T.N. Trnka, J.B. Bonanno, B.M. Bridgewater, G. Parkin, Organometallics 20 (2001) 3255.
[10] J.S. Overby, T.P. Hanusa, P.D. Boyle, Angew. Chem. Int. Ed. Engl. 36 (1997) 2378.
[11] M.J. Frisch, G.W. Trucks, H.B. Schlegel, G.E. Scuseria, M.A. Robb, J.R. Cheeseman, V.G. Zakrzewski, J.A. Montgomery Jr., R.E. Stratmann, J.C. Burant, S. Dapprich, J.M. Millam, A.D. Daniels, K.N. Kudin, M.C. Strain, O. Farkas, J. Tomasi, V. Barone, M. Cossi, R. Cammi, B. Mennucci, C. Pomelli, C. Adamo, S. Clifford, J. Ochterski, G.A. Petersson, P.Y. Ayala, Q. Cui, K. Morokuma, D.K. Malick, A.D. Rabuck, K. Raghavachari, J.B. Foresman, J. Cioslowski, J.V. Ortiz, B.B. Stefanov, G. Liu, A. Liashenko, P. Piskorz, I. Komaromi, R. Gomperts, R.L. Martin, D.J. Fox, T. Keith, M.A. Al-Laham, C.Y. Peng, A. Nanayakkara, C. Gonzalez, M. Challacombe, P.M.W. Gill, B. Johnson, W. Chen, M.W. Wong, J.L. Andres, C. Gonzalez, M. Head-Gordon, E.S. Replogle, J.A. Pople, GAUSSIAN-98, Revision A.6, Gaussian, Inc., Pittsburgh, PA, 1998.
[12] J.D. Smith, T.P. Hanusa, Organometallics 20 (2001) 3056.
[13] D. O'Hare, V.J. Murphy, N. Kaltsoyannis, J. Chem. Soc. Dalton Trans. (1993) 383.
[14] J.S. Overby, T.P. Hanusa, S.P. Sellers, G.T. Yee, Organometallics 18 (1999) 3561.
[15] (a) E.J. Baerends, A. Bérces, C. Bo, P.M. Boerrigter, L. Cavallo, L. Deng, R.M. Dickson, D.E. Ellis, L. Fan, T.H. Fischer, C. Fonseca Guerra, S.J.A. van Gisbergen, J.A. Groeneveld, O.V. Gritsenko, F.E. Harris, P. van den Hoek, H. Jacobsen, G. van Kessel, F. Kootstra, E. van Lenthe, V.P. Osinga, P.H.T. Philipsen, D. Post, C.C. Pye, W. Ravenek, P. Ros, P.R.T. Schipper, G. Schreckenbach, J.G. Snijders, M. Sola, D. Swerhone, G. te Velde, P. Vernooijs, L. Versluis, O. Visser, E. van Wezenbeek, G. Wiesenekker, S.K. Wolff, T.K. Woo, T. Ziegler, ADF, 2000;
(b) C. Fonseca Guerra, O. Visser, J.G. Snijders, G. te Velde, E.J. Baerends, Parallelisation of the Amsterdam density functional programme, in: E. Clementi, C. Corongiu (Eds.), Methods and Techniques for Computational Chemistry, STEF, Cagliari, 1995, pp. 303–395;
(c) C. Fonseca Guerra, J.G. Snijders, G. te Velde, E.J. Baerends, Theor. Chem. Acc. 99 (1998) 391;
(d) E.J. Baerends, D. Ellis, P. Ros, Chem. Phys. 2 (1973) 41;
(e) E.J. Baerends, P. Ros, Int. J. Quantum Chem. S12 (1978) 169;
(f) P.M. Boerrigter, G. te Velde, E.J. Baerends, Int. J. Quantum

Chem. 33 (1988) 87;
(g) G. te Velde, E.J. Baerends, J. Comp. Phys. 99 (1992) 84.
[16] O. Heinemann, P.W. Jolly, C. Krüger, G.P.J. Verhovnik, Organometallics 15 (1996) 5462.
[17] C.C. Romão, V. Félix, B. Royo, M.G.B. Drew, J. Chem. Soc. Dalton (2002) 584.
[18] A.N. Nesmeyanov, N.A. Ustyniuk, L.G. Makarova, V.G. Andrianov, Yu.T. Struchkov, S. Andrae, J. Organomet. Chem. 159 (1978) 189.
[19] A.K. Rappé, C.J. Casewit, K.S. Colwell, W.A. Goddard, III, W.M. Skiff, J. Am. Chem. Soc. 114 (1992) 10024.
[20] CERIUS2, version 3.5, Molecular Simulations Inc, San Diego, 1997.
[21] M. Widhalm, U. Nettekoven, H. Kalchhauser, K. Mereiter, M.J. Calhorda, V. Félix, Organometallics 315 (2002) 21.
[22] (a) R. Hoffmann, J. Chem. Phys. 39 (1963) 1397;
(b) R. Hoffmann, W.N. Lipscomb, J. Chem. Phys. 36 (1962) 2179.
[23] C. Mealli, D.M. Proserpio, J. Chem. Educ. 67 (1990) 39.
[24] S.H. Vosko, L. Wilk, M. Nusair, Can. J. Phys. 58 (1980) 1200.
[25] (a) L. Versluis, T. Ziegler, J. Chem. Phys. 88 (1988) 322;
(b) L. Fan, T. Ziegler, J. Chem. Phys. 95 (1991) 7401.
[26] A.D. Becke, J. Chem. Phys. 88 (1987) 1053.
[27] (a) J.P. Perdew, Phys. Rev. B33 (1986) 8822;
(b) J.P. Perdew, Phys. Rev. B34 (1986) 7406.
[28] (a) T.H. Dunning, Jr., P.J. Hay, in: H.F. Schaefer, III (Ed.), Modern Theoretical Chemistry, vol. 3, Plenum, New York, 1976, p. 1;
(b) P.J. Hay, W.R. Wadt, J. Chem. Phys. 82 (1985) 270;
(c) W.R. Wadt, P.J. Hay, J. Chem. Phys. 82 (1985) 284;
(d) P.J. Hay, W.R. Wadt, J. Chem. Phys. 82 (1985) 2299.
[29] W.J. Hehre, L. Radom, P.v.R. Schleyer, J.A. Pople, Ab Initio Molecular Orbital Theory, John Wiley & Sons, New York, 1986.
[30] A.D. Becke, J. Chem. Phys. 98 (1993) 5648.
[31] (a) C. Lee, W. Yang, R.G. Parr, Phys. Rev. B 37 (1988) 785;
(b) B. Miehlich, A. Savin, H. Stoll, H. Preuss, Chem. Phys. Lett. 157 (1989) 200.
[32] J.H. Ammeter, H.-J. Bürgi, J.C. Thibeault, R. Hoffmann, J. Am. Chem. Soc. 100 (1978) 3686.